Symmetry, invariance and the structure of matter

Richard D. James

Department of Aerospace Engineering and Mechanics
University of Minnesota
james@umn.edu

Abstract. We present a mathematical view of the structure of matter based on the invariance of the classical equations of physics.

Contents

1 Symmetry and invariance

Physicists and mathematicians have long tried to understand the structure of matter from a deductive viewpoint. Early examples are Hooke's Micrographia [28] and, inspired in part by microscopic observations, Euler's "Physical investigations on the nature of the smallest parts of matter" [16]. As the incredible difficulty of achieving rigorous results in this direction

became better appreciated, the problem was narrowed to the "crystallization problem": that is, prove for the simplest models of atomic forces that the Face-Centered Cubic lattice (FCC, defined below) minimizes the potential energy. Inspired by the seminal work of Radin [25] and also relying on recent advances in the calculus of variations, research on the crystallization problem has achieved significant advances [23, 40, 19]. In these works the symmetry of the FCC lattice and the invariance of the underlying equations play a dominant role.

Our purpose is not to survey these advances, but rather to broaden the discussion by collecting a list of examples in which structure and invariance are intimately related. There are three benefits: 1) a treasure trove of interesting mathematical problems is revealed, 2) modern research on nanoscience is given a mathematical perspective, and 2) one realizes that the subject is more about invariance than structure.

2   The Periodic Table

We start at the most basic level: the Periodic Table of the elements. Most people think of the crystal structures of the elements in terms of Bravais lattices, and the standard databases are organized on this basis. A Bravais lattice is the infinite set of points $\mathcal{L}(e_1, e_2, e_3) = \{\nu^1 e_1 + \nu^2 e_2 + \nu^3 e_3 : (\nu^1, \nu^2, \nu^3) \in \mathbb{Z}^3\}$, where e_1, e_2, e_3 are linearly independent vectors in $\mathbb{R}^3$ called *lattice vectors*.

For example, consider lattice vectors $e_1 = \alpha \hat{e}_1, e_2 = \alpha \hat{e}_2$ and $e_3 = \alpha(\hat{e}_1 + \hat{e}_2 + \gamma \hat{e}_3)/2$ where $\hat{e}_1, \hat{e}_2, \hat{e}_3 = \hat{e}_1 \times \hat{e}_2$ are orthonormal and $\alpha, \gamma > 0$. The constants α, γ that quantify the distances between atoms are called *lattice parameters*. The value $\gamma = 1$ gives the Body-Centered Cubic (BCC) lattice. A famous observation of Bain [1] is that there is exactly one other choice of $\gamma > 0$ in which the associated Bravais lattice has cubic symmetry, that being $\gamma = \sqrt{2}$, which in fact gives the FCC lattice. About half of the Periodic Table consists of elements whose normal crystal structure at room temperature is either BCC or FCC. In fact, Bain theorized that best represented phase transformation in the Periodic Table, BCC→FCC, is achieved by passing γ from 1 to $\sqrt{2}$.

How about the other half? To discuss this more precisely, let us remove the last row of the Periodic Table, atomic numbers 87-118, which are typically radioactive and often highly unstable, and also number 85 (Astatine), for which there exists much less than 1 gram in the earth's crust at any one time and cannot be considered to have a bulk crystal structure. For definiteness, we take the accepted most common crystal structure at room temperature, unless the material is not solid at room temperature, in which case we take the accepted structure at zero temperature. Many (but not all) of the other half are 2-lattices, i.e., the union of two displaced Bravais lattices made with the same lattice vectors:

$$\{a + \mathcal{L}(e_1, e_2, e_3)\} \cup \{b + \mathcal{L}(e_1, e_2, e_3)\}, \tag{1}$$

where $a \neq b \in \mathbb{R}^3$, or equivalently, the periodic extension of two atomic positions a, b using the periodicity e_1, e_2, e_3. For example, the third most prominent structure in the Periodic Table is the Hexagonal Close Packed (HCP) lattice for which we can choose $e_1 = \sqrt{3}\alpha \hat{e}_1$, $e_2 = \sqrt{3}\alpha\big((1/2)\hat{e}_1 + (\sqrt{3}/2)\hat{e}_2\big)$, $e_3 = 2\alpha\sqrt{2}\hat{e}_3$ and, for example, $a = 0$, $b = \alpha\hat{e}_2 + \sqrt{2}\alpha\hat{e}_3$. Clearly, HCP is not a Bravais lattice, since $a + 2(b - a) = 2b$ does not belong to (1). HCP accounts for about 1/5 of the Periodic Table. Silicon and germanium (and carbon) adopt the diamond

structure under ordinary conditions, which is also a 2-lattice. Many layered compounds such as the halogens, carbon (as graphite), oxygen and nitrogen are also 2-lattices, either as individual layers or as their accepted layered structures. Altogether, about 1/4 of the elements in the Periodic Table are 2-lattices. There are also examples that are not crystals at all under ordinary conditions, such as sulfur (a double ring) and boron (icosahedra, sometimes weakly bonded).

Even if they are not common, we also should mention the celebrated structures of nanotechnology: graphene, carbon nanotubes, the fullerines, phosphorene, and the many other 2D materials now under study.

We will explore an alternative way of looking at the Periodic Table, and structure in general, via the concept of *objective strutures* [31]. In fact the examples mentioned above have a common mathematical structure not based on Bravais lattices. An *objective atomic structure* (briefly, a 1-OS) has the defining property that each atom "sees the same environment". Imagine Maxwell's demon, sitting on an atom, and looking at the environment (out to infinity). The demon hops to another atom, reorients itself in a certain way, and sees exactly the same environment. Mathematically, a set of points in $\mathbb{R}^3$ is given, $\mathcal{S} = \{x_1, x_2, \ldots, x_N\} \in (R^3)^N$, $N \leq \infty$ (most of the structures mentioned above are infinite). $\mathcal{S}$ is a 1-OS if there are orthogonal transformations $Q_1, \ldots, Q_N$ such that

$$\{x_i + Q_i(x_j - x_1) : j = 1, \ldots, N\} = \mathcal{S} \quad \text{for} \quad i = 1, \ldots, N. \tag{2}$$

Again, in words, the structure as viewed from atom 1, $x_j - x_1$, undergoes an orthogonal transformation $Q_i(x_j - x_1)$ depending on i, is added back to atom i, $x_i + Q_i(x_j - x_1)$, and the structure is restored. The surprising fact is that nearly all of the structures mentioned above, including the 2-lattices and those workhorse structures of nanotechnology, are examples of 1-OS.

It is indeed surprising. One would expect that identical environments would require some kind of isotropy of atomistic forces (for example, pair potentials, with force between a pair depending only on the distance). But some of the examples above are covalently bonded with complex electronic structure [3]. Evidently, the property of identical environments is not coincidental. Unsurprisingly, many useful necessary conditions about equilibrium and stability follow from the definition [31]. However, the basic reason why these structures are so common can be considered one of the fundamental open questions of atomic structure.

There is a glaring counter-example: atomic number 25, Manganese. In fact, this "most complex of all metallic elements"[27] is (at room temperature and pressure) a 4-lattice. According to Hobbs et al. [27], due to nearly degenerate spin configurations, the observed structure should be considered as containing four different magnetic atoms MnI, MnII, MnIII, MnIV. Briefly, Mn should be considered an alloy, rather than an element. There are a few other cases that could be considered equivocal: Is the structure of boron icosahedral (a 1-OS) or the weakly bonded lattice of icosahedra (not a 1-OS) that is sometimes given as its structure? But, overwhelmingly, the assertion made above about the prevalence of 1-OS on both the Periodic Table, and also for nanostructures made with one type of atom, is accurate.

Intuitively, one can easily imagine why such structures are interesting. If a property can be assigned to each atom, depending on its environment, it is *frame-indifferent* (independent of the Q_i), and one can superpose it by summing over atoms, then an appreciable bulk property

3

could result. This property, and fact that the patterns of bonding that in nanostructures differ appreciably those from bulk crystals, underlies significant research in nanoscience.

The idea of objective structures was articulated by Crick and Watson [10], Caspar and Klug [5] and in the less well-known work of Crane [9]. Caspar and Klug used the term *equivalence* to denote structures in which each subunit is "situated in the same environment". The fundamental paper of Dolbilin, Lagarias and Senechal [13] proposed the concept of *regular point systems*, which adds to the idea of identical environments the hypotheses of uniform discreteness and relative denseness.

3   Objective structures

Structures containing only one element are interesting, but very special. There is a more general concept [31] applicable to the structures of many alloys and many molecular structures. Consider a structure consisting of N "molecules", each consisting of M atoms. The terminology is for convenience – they may not be actual molecules. We say that a structure is an *objective molecular structure* (briefly, an M-OS) if one can set up a one-to-one correspondence between atoms in each molecule such that equivalent atoms see that same environment. So, in this case we use a double-index notation $\mathcal{S} = \{x_{i,k} \in \mathbb{R}^3 : i = 1, \ldots, N, \ k = 1, \ldots, M\}$, where $x_{i,k}$ is the position of atom k in molecule i. Here, with $N \leq \infty$ and $M < \infty$. $\mathcal{S}$ is an M-OS if $x_{1,1}, \ldots x_{1,M}$ are distinct and there are NM orthogonal transformations $Q_{i,k}, \ i = 1, \ldots, N, \ k = 1, \ldots, M$ such that

$$\{x_{i,k} + Q_{i,k}(x_{j,\ell} - x_{1,k}) : j = 1, \ldots, N, \ \ell = 1, \ldots, M\} = \mathcal{S} \quad \text{for} \ \ i = 1, \ldots, N, \ k = 1, \ldots, M. \tag{3}$$

Note that the reorientation $Q_{i,k} \in O(3)$ is allowed to depend on both i and k. Briefly, $x_{i,k}$ sees the same environment as $x_{1,k}$. This definition is the direct analog of *multiregular point systems* of Dolbilin, Lagarias and Senechal [13], but excluding the conditions of uniform discreteness and relative denseness. The author was led to it in a study with Falk [17] of the helical tail sheath of Bacteriophage T-4, while writing a formula for the positions and orientations of its molecules consistent with measured electron density maps. An M-OS$|_{M=1}$ is a 1-OS.

The definition of an M-OS can be written using a permutation Π on two indices $(p, q) = \Pi(j, \ell)$:

$$x_{i,k} + Q_{i,k}(x_{j,\ell} - x_{1,k}) = x_{\Pi(j,\ell)}. \tag{4}$$

It is not reflected by the notation here, but Π depends on the choice of (i, k). We can also assign a species to each (j, ℓ). In most applications it would be required that atom (j, ℓ) is the same species as atom (j', ℓ). Also, it would be required that Π preserve species, so that the environment of atom (i, k) matches the environment of atom $(1, k)$ in both placement and species of atoms. The most interesting dimensions for the structure of matter are 3 and 2, but the definition is meaningful in any number of dimensions. Finally, in applications to atomic structure we are only interested in discrete M-OS. Of course, if one point of a 1-OS is an accumulation point, then every point is an accumulation point, since each point sees the same environment.

The assertions about 1-OS made in the preceding section are easily proved using the definitions above, but an even easier method is to note the following relation between objec-

tive structures and isometry groups. An isometry group is a group of elements of the form $(Q|c)$, $Q \in O(n)$, $c \in \mathbb{R}^n$ based on the product $(Q_1|c_1)(Q_2|c_2) = (Q_1Q_2|c_1 + Q_1c_2)$, the identity $(I|0)$, and inverses $(Q|c)^{-1} = (Q^T| - Q^Tc)$. Isometries can act on $\mathbb{R}^n$ in the obvious way: $g(x) = Qx + c$ where $g = (Q|c)$. The product is designed to agree with composition of mappings: $g_1g_2(x) = g_1(g_2(x))$. As above, in view of the applications, we will put $n = 3$.

Let $\mathcal{S} = \{x_{i,k} \in \mathbb{R}^3 : i = 1, \ldots, N, \ k = 1, \ldots, M\}$ be a discrete M-OS. Any such structure has an isometry group G:

$$G = \{(Q|c), Q \in O(3), c \in \mathbb{R}^3 : Qx_{i,k} + c = x_{\Pi(i,k)} \text{ for a permutation } \Pi\}. \tag{5}$$

Let $\mathcal{M}_1 = \{x_{1,k} : k = 1, \ldots, M\}$ be "molecule 1". We wish to show that $\mathcal{S}$ is the orbit of molecule 1 under a discrete group of isometries. To see this, rearrange the definition of an M-OS as

$$R_{i,k}x_{j,\ell} + x_{i,k} - R_{i,k}x_{1,k} = x_{\Pi(j,\ell)}. \tag{6}$$

Hence, $g_{i,k} := (R_{i,k} \, | \, x_{i,k} - R_{i,k}x_{1,k}) \in G$. However, trivially, $g_{i,k}(x_{1,k}) = x_{i,k}$, and this holds for all $i = 1, \ldots, N$, $k = 1, \ldots, M$. Hence, $\mathcal{S}$ is contained in the orbit of $\mathcal{M}_1$ under G. Conversely, putting $i = 1$ in (5) we have that the orbit of $\mathcal{M}_1$ under G is contained in $\mathcal{S}$.

This simple argument apparently has two flaws. First, the group G that one gets may not be discrete. That would be a serious flaw, since evidently we know very little about the nondiscrete groups of isometries, even in $\mathbb{R}^3$. (However, see remarks below for why these groups might be important to the structure of matter.) We should mention that discreteness is not merely a technical condition that rules out some special cases, but rather it plays a dominant role in the derivation of the groups, particularly in the subperiodic case appropriate to nanostructures. Second, in this argument there is nothing that prevents the images of $\mathcal{M}_1$ from overlapping. The latter is consistent with the definitions, and also advantageous from the physical viewpoint. That is, while we have imposed the condition that the points in $\mathcal{M}_1$ are distinct, the definition of M-OS allows $x_{i,j} = x_{i',j}$ for $i \neq i'$. This is advantageous as it saves the result above. Also, it allows a structure such as ethane C_2H_6 to be a 2-OS, which is certainly reasonable: $\mathcal{M}_1$ is C-H, each H sees the same environment, each C sees the same environment, and the image of C-H has overlapping Cs.

The geometric concept of identical environments allows $Q_{i,k}$ to depend on both i, k. However, if $\mathcal{S}$ is the orbit of $x_{1,k}$, $k = 1, \ldots, M$, under an isometry group $g_1 = (Q_1|c_1), \ldots, g_N = (Q_N|c_N)$, i.e., $x_{i,k} = Q_i x_{1,k} + c_c$, then $Q_{i,k}$ in (3) can be chosen as Q_i, and thus is independent of k. This is seen by direct substitution of $Q_{i,k} = Q_i$ into (3).

The nondiscreteness turns out not to be a problem. It is easily proved that if a nondiscrete group of isometries in 3-D generates a discrete structure when applied to a point x_1, it gives a single point, a 1-D Bravais lattice, or a 1-D 2-lattice.

Now we can revisit some of the assertions make in Section 2 concerning examples of 1-OS.

Buckminsterfullerine (C_{60}) Let $G = \{R_1, \ldots, R_N\}$ be a finite subgroup of $O(3)$ and $x_1 \neq 0$. (For C_{60} choose the icosahedral group, $N = 60$) and let $x_i = R_i x_1$, $i = 1, \ldots, N$. One can also see directly that (2) is satisfied with $Q_i = R_i$. In case that x_1 is fixed by some elements of $R_1, \ldots, R_N$, then in this case one can replace G by G/G_{x_1} to obtain a free action (i.e., avoid duplication).

Single-walled carbon nanotubes (of any chirality)
The formulas below can be found by rolling up a graphene sheet isometrically and seamlessly (see, e.g., [14]) and then noticing the group structure. The positive integers (n, m) define the *chirality*. Letting $\hat{e}_1, \hat{e}_2, \hat{e}_3$ be an orthonormal basis and $R_\theta \in \mathrm{SO}(3)$ a rotation with counterclockwise angle θ and axis $\hat{e}_3$, carbon nanotubes are given by the formula

$$g_1^{\nu_1} g_2^{\nu_2} g_3^{\nu_3}(x_1), \quad \nu_1, \nu_2, \nu_3 \in \mathbb{Z}, \tag{7}$$

with $g_1 = (R_{\theta_1}|t_1), g_2 = (R_{\theta_2}|t_2)$ and $g_3 = (-I + 2e \otimes e \,|0)$,

Figure 1: Buckminsterfullerine. Pentagons added for clarity.

$$t_1 = \tau_1 \hat{e}_3, \quad t_2 = \tau_2 \hat{e}_3, \quad e = \cos(\pi\xi)\hat{e}_1 + \sin(\pi\xi)\hat{e}_2, \quad x_1 = \rho\hat{e}_1 - \eta\hat{e}_3, \tag{8}$$

and

$$
\begin{aligned}
\theta_1 &= \frac{\pi(2n+m)}{n^2+m^2+nm}, \quad \theta_2 = \frac{\pi(2m+n)}{n^2+m^2+nm}, \quad \tau_1 = \frac{3m\ell_{C-C}}{2\sqrt{n^2+m^2+nm}}, \quad \tau_2 = \frac{-3n\ell_{C-C}}{2\sqrt{n^2+m^2+nm}}, \\
\xi &= \frac{(2n+m)+(2m+n)}{6(n^2+m^2+nm)}, \quad \rho = \frac{\ell_{C-C}}{2\pi}\sqrt{3(n^2+m^2+nm)}, \quad \eta = \frac{\ell_{C-C}(m-n)}{4\sqrt{n^2+m^2+nm}}. \tag{9}
\end{aligned}
$$

The fixed integers n, m define the chirality of the nanotube and ℓ_{C-C} is the carbon-carbon bond length before rolling (To account for additional relaxation of the bond lengths after rolling one can simply omit the formula for the radius ρ and treat ρ as an independent parameter).

We see that $g_1 g_2 = g_2 g_1$ and $g_i g_3 = g_3 g_i^{-1}, i = 1, 2$, so $g_1^{\nu_1} g_2^{\nu_2} g_3^{\nu_3}, \nu_1, \nu_2, \nu_3 \in \mathbb{Z}$ is a (discrete) group. Therefore the orbit (7) describes a 1-OS. To obtain a free action, confine $\nu_3 \in \{1, 2\}$, $\nu_1 \in \mathbb{Z}$ and $\nu_2 \in \{1, \ldots, \nu_\star\}$, where $\nu_\star$ is the smallest positive integer such that $g_1^\nu g_2^{\nu_\star} = id$ is solvable for $\nu \in \mathbb{Z}$.

Figure 2: Carbon nanotube (a 1-OS) with chirality $n = 3$, $m = 8$, $\ell_{C-C} = 1.42$, colored according to the value of $\nu_3 \in \{1, 2\}$.

Any 2-lattice Of course any Bravais lattice is a 1-OS: use a suitable indexing in terms of triples of integers $\nu = (\nu^1, \nu^2, \nu^3)$, write $x_\nu = \nu^1 e_1 + \nu^2 e_2 + \nu^3 e_3$ and choose $Q_\nu = I$ in (2). As noted above and represented prominently in the Periodic Table, any 2-lattice is also a 1-OS. To see this, choose $g_1 = (I\,|e_1)$, $g_2 = (I\,|e_2)$, $g_3 = (I\,|e_3)$ and $g_4 = (-I\,|0)$. Then, for $s = 1, 2$,

$$g_1^{\nu_1} g_2^{\nu_2} g_3^{\nu_3} g_4^s(x_1) = \nu^1 e_1 + \nu^2 e_2 + \nu^3 e_3 \pm x_1. \tag{10}$$

Referring to (1) we can choose $x_1 = (b-a)/2$ and modify these isometries to translate the whole structure[1] by $(a+b)/2$ to get exactly (1). Of course, $\{g_1^{\nu_1} g_2^{\nu_2} g_3^{\nu_3} g_4^s : \nu_1, \nu_2, \nu_3 \in \mathbb{Z}^3, s = 1, 2\}$ is a (discrete) group, because g_1, g_2, g_3 commute and $g_i g_4 = g_4 g_i^{-1}, i = 1, 2, 3$.

This kind of argument works in any number of dimensions and therefore covers two-dimensional 2-lattices, such as graphene.

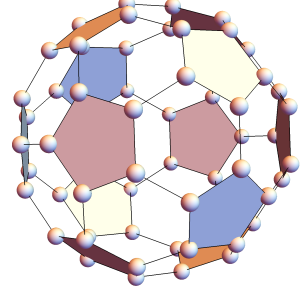[1] Change each g_i to $t g_i t^{-1}$ where $t = (I|c)$, $c = (a+b)/2$.

HCP   The hexagonal close packed lattice is a 2-lattice, as proved above,
and therefore is a 1-OS by the result just above. However, it is useful to express it by a different group to expose an important issue. Beginning from the description HCP above, i.e.,

$$e_1 = \sqrt{3}\alpha\hat{e}_1, \;\; e_2 = \sqrt{3}\alpha\big((1/2)\hat{e}_1 + (\sqrt{3}/2)\hat{e}_2\big), \;\; e_3 = 2\alpha\sqrt{2}\hat{e}_3, \tag{11}$$

and with $R_\theta \in \mathrm{SO}(3)$ a counterclockwise rotation of θ about $\hat{e}_3$, define

$$h = (R_{\pi/3}\,|\,(1/2)e_3), \;\; t_1 = (I\,|\,e_1) \;\; t_2 = (I\,|\,e_2). \tag{12}$$

The set $\{h^i g_1^j g_2^k : i, j, k \in \mathbb{Z}\}$ is a group $(t_1 t_2 = t_2 t_1, \; t_2 h = h t_1, \; t_1 h = h t_1 t_2^{-1})$, and the orbit of $(2/3)e_2 - (1/3)e_1$ is HCP. This illustrates that we can have two groups, this one and the one of the preceding paragraph, not related by an affine transformation $G \to aGa^{-1}$, $a = (A|c), \det A \neq 0$, that generate the same structure when the orbits of suitable points are taken.

   For the purpose of this article we do not care about multiplication tables (we need the actual isometries with their parameter dependence), affine equivalence (example of HCP) or whether the closure of the fundamental domain is compact (not true for nanostructures). Embarrassingly, we do not even care much about symmetry. If we have a set of generators, depending smoothly on parameters, and the symmetry suddenly jumps up at values of the parameters – such as at $\gamma = 1, \sqrt{2}$ in the example of Bain above – it makes no difference for any of the results given below. On the other hand, the analytical structure of the generators is critically important. For the purposes here it would be very useful to have a short lists of formulas for generators giving all objective structures, not further broken down according to their abstract groups.

4   An invariant manifold of molecular dynamics

Structure and invariance come together when we assign a set of differential equations having an invariance group that matches the group used to make the structure. Isometries are expected to play an important role because of the frame-indifference of atomic forces. Examples of exploiting symmetries in continuum theory [15] might suggest that a differential structure (i.e, a Lie group) is essential, but, in fact, the matching of discrete group and discrete structure is also possible.

   Molecular dynamics is an interesting example. The basic invariance of the equations of molecular dynamics is frame-indifference and permutation invariance. Let us use the indexing of M-OS to describe these invariances, but without any assumptions about the structure. So we assume a collection of atomic positions $\mathcal{S} = \{x_{i,k} \in \mathbb{R}^3 : i = 1, \ldots, N, \; k = 1, \ldots, M\}$ with $N \leq \infty$ and $M < \infty$, and suppose that the force on atom (i, k) is given by

$$f_{i,k}(\ldots, x_{j,1}, x_{j,2}, \ldots, x_{j,M}, x_{j+1,1}, x_{j+1,2}, \ldots, x_{j+1,M}, \ldots). \tag{13}$$

As indicated, the force on atom (i, k) depends on the positions of all the atoms. We have NM such forces. They are subject to two fundamental invariances: frame-indifference and permutation invariance.

Frame-indifference. For $Q \in O(3)$, $c \in \mathbb{R}^3$,

$$f_{i,k}(\ldots, Qx_{j,1} + c, \ldots, Qx_{j,M} + c, Qx_{j+1,1} + c, \ldots, Qx_{j+1,M} + c, \ldots) \qquad (14)$$
$$= Qf_{i,k}(\ldots, x_{j,1}, \ldots, x_{j,M}, x_{j+1,1}, \ldots, x_{j+1,M}, \ldots),$$

for all $Q \in \mathrm{O}(3)$, $c \in \mathbb{R}^3$ and $x_{j,\ell} \in (R^3)^{NM}$.

Permutation invariance. For all permutations Π and $x_{j,\ell} \in (R^3)^{NM}$,

$$f_{i,k}(\ldots, x_{\Pi(j,1)} \ldots, x_{\Pi(j,M)}, x_{\Pi(j+1,1)}, \ldots, x_{\Pi(j+1,M)}, \ldots) \qquad (15)$$
$$= f_{\Pi(i,k)}(\ldots, x_{j,1}, \ldots, x_{j,M}, x_{j+1,1}, \ldots, x_{j+1,M}, \ldots),$$

If we introduce species as described above, then Π is also required to preserve species: if atom i, k has species $\mathcal{A}$ and $(p, q) = \Pi(i, k)$ then the species of atom p, q is $\mathcal{A}$.

Typically, $NM = \infty$, in which case one cannot speak of a potential energy, but, in the finite case, if $f_{i,k} = -\partial\varphi/\partial x_{i,k}$ then the conditions (15), (16) follow from the familiar invariances $\varphi(\ldots, Qx_{j,\ell} + c, \ldots) = \varphi(\ldots, x_{j,\ell}, \ldots)$ and $\varphi(\ldots, x_{\Pi(j,\ell)}, \ldots) = \varphi(\ldots, x_{j,\ell}, \ldots)$, respectively.

As one can see from the examples (7)-(12), the formulas for objective structures contain lots of parameters. Eventually, we are going to solve the equations of molecular dynamics for functions depending on time, $t > 0$. To use the invariance as completely as possible without unduly restricting the number of atoms or their motions, we could allow these group parameters to depend on time. In general suppose we have an isometry group $g_1 = (Q_1(t) | c_1(t)), \ldots, g_N = (Q_N(t) | c_N(t))$ smoothly depending on t. The property we will need is

$$\frac{d^2}{dt^2} g_i(y(t)) = \frac{d^2}{dt^2}\big(Q_i(t)y(t) + c_i(t)\big) = Q_i(t)\frac{d^2 y(t)}{dt^2}, \qquad (16)$$

but we will know very little *a priori* about $y(t), t > 0$, beyond some smoothness. Letting a superimposed dot indicate the time derivative and using $\dot{Q}_i = Q_i W_i$, where $W_i^T = -W_i$, the condition (16) is

$$\ddot{c}_i = -Q_i\big(W_i^2 y + \dot{W}_i y + 2W_i \dot{y}\big). \qquad (17)$$

The only way this holds for any reasonable class[2] of smooth motions $y(t)$ is

$$Q_i = const. \in \mathrm{O}(3) \quad \text{and} \quad c_i = a_i t + b_i, \qquad (18)$$

where $a_i, b_i \in \mathbb{R}^3$, $i = 1, \ldots, N$. While the latter may appear to be merely a Galilean transformation, the dependence on i gives many nontrivial cases. Of course, one has to check that the (18) is consistent with the group properties at each $t > 0$.

We say that the group $G = \{g_1, \ldots, g_N\}$, $g_i = (Q_i | a_i t + b_i)$, is a *time-dependent discrete group of isometries* if (18) is satisfied, and we use the notation $g_i(y, t) = Q_i y + a_i t + b_i$. We also assign a mass $m_k > 0$ to each atom $(1, 1), \ldots (1, M)$, and we assume that atom i, k also has mass m_k, consistent with the remarks about species above. Now, instead of thinking of atoms $(1, 1), \ldots (1, M)$ as molecule 1, we think in terms of a numerical method, and call atoms $(1, 1), \ldots (1, M)$ the *simulated atoms*. In many cases they will not behave at all like a

---

[2]It is not sufficient for our purposes to satisfy (17) in a statistical sense.

molecule. We will also have *nonsimulated atoms* and their positions will be given (as in an M-OS) by the group:

$$y_{i,k}(t) = g_i(y_{1,k}(t), t), \quad i = 1, \ldots, N, \quad k = 1, \ldots, M \tag{19}$$

Obviously we have assigned $g_1 = id$.

Let $G = \{g_1, \ldots, g_N\}$ *be a time-dependent discrete group of isometries. Let initial positions* $y_k^\circ \in \mathbb{R}^3$ *and initial velocities* v_k°, $k = 1, \ldots, M$, *be given and suppose the simulated atoms* $y_{1,k}(t), t > 0$, *satisfy the equations of molecular dynamics for forces that are frame-indifferent and permutation invariant:*

$$
\begin{aligned}
m_k \ddot{y}_{1,k} &= f_{1,k}(\ldots, y_{j,1}, y_{j,2}, \ldots, y_{j,M}, y_{j+1,1}, y_{j+1,2}, \ldots, y_{j+1,M}, \ldots) \\
&= f_{1,k}(\ldots, g_j(y_{1,1}, t), \ldots, g_j(y_{1,M}, t), g_{j+1}(y_{1,1}, t), \ldots, g_{j+1}(y_{1,M}, t), \ldots), \tag{20}
\end{aligned}
$$

subject to the initial conditions

$$y_{1,k}(0) = y_k^\circ, \quad \dot{y}_{1,k}(0) = v_k^\circ, \quad k = 1, \ldots, M. \tag{21}$$

Then, the nonsimulated atoms also satisfy the equations of molecular dynamics:

$$m_k \ddot{y}_{i,k} = f_{1,k}(\ldots, y_{j,1}, y_{j,2}, \ldots, y_{j,M}, y_{j+1,1}, y_{j+1,2}, \ldots, y_{j+1,M}, \ldots). \tag{22}$$

Note that (20),(21) is a (nonautonomous) system of ODEs in standard form for the simulated atoms. We have not stated this as a theorem because we have not spelled out the (straightforward) conditions on $f_{1,k}$ that would allow us to invoke one of the standard existence theorems of ODE theory. Another (also straightforward to handle) technical issue is that a standard atomic forces blow up repulsively when two atoms approach each other. Aside from these issues, the proof is a simple calculation that uses both frame-indifference and permutation invariance. To see this, fix i, k and suppose we want to prove that $y_{i,k}(t)$ satisfies (22) as written. Write $g_i = (Q_i \,|\, c_i)$, $c_i = a_i t + b_i$, so that $g_i^{-1} = (Q^T \,|\, -Q^T c_i)$. There is a permutation Π (depending on i) such that $y_{\Pi(j,\ell)}(t) = g_i^{-1}(y_{j,\ell}, t)$. This permutation satisfies $\Pi(i, k) = (1, k)$. Now use (16), permutation invariance, and frame-indifference (in that order):

$$
\begin{aligned}
m_k \ddot{y}_{i,k} = m_k Q_i \ddot{y}_{1,k} &= Q_i f_{1,k}(\ldots, y_{j,1}, \ldots, y_{j,m}, y_{j+1,1}, \ldots, y_{j+1,M}, \ldots) \\
&= Q_i f_{\Pi(i,k)}(\ldots, y_{j,1}, \ldots, y_{j,m}, y_{j+1,1}, \ldots, y_{j+1,M}, \ldots) \\
&= Q_i f_{i,k}(\ldots, y_{\Pi(j,1)}, \ldots, y_{\Pi(j,m)}, y_{\Pi(j+1,1)}, \ldots, y_{\Pi(j+1,M)}, \ldots) \\
&= Q_i f_{i,k}(\ldots, g_i^{-1}(y_{j,1}), \ldots, g_i^{-1}(y_{j,m}), g_i^{-1}(y_{j+1,1}), \ldots, g_i^{-1}(y_{j+1,M}), \ldots) \\
&= Q_i f_{i,k}(\ldots, Q_i^T(y_{j,1} - c_i), \ldots, Q_i^T(y_{j,m} - c_i), Q_i^T(y_{j+1,1} - c_i), \\
&\qquad\qquad\qquad\qquad\qquad \ldots, Q_i^T(y_{j+1,M} - c_i), \ldots) \\
&= f_{i,k}(\ldots, y_{j,1}, \ldots, y_{j,m}, y_{j+1,1}, \ldots, y_{j+1,M}, \ldots). \tag{23}
\end{aligned}
$$

This result can be rephrased as the existence of a (time-dependent) invariant manifold of molecular dynamics. Given the many isometry groups and their time dependences, this provides a multitude of mainly unstudied invariant manifolds of the equations of molecular dynamics. Their stability of course is also unknown.

9

We can describe these invariant manifolds in terms of the isometry groups. The conventional description is in phase space, using momenta $p_{i,k} = m_k \dot{y}_{i,k}$ and positions $q_{i,k} = y_{i,k}$. Using our notation for time-dependent discrete isometry groups, $G = \{g_1, \ldots, g_N\}$, $g_i = (Q_i \,|\, a_i t + b_i)$, we observe that

$$p_{i,k} = Q_i p_{1,k} + m_k a_i, \quad q_{i,k} = Q_i q_{1,k} + a_i t + b_i, \tag{24}$$

which describes an affine manifold in phase space with a simple affine time dependence. Except for the trivial m_k dependence in the first of (24), this family of invariant manifolds *is independent of the material*. That is, this large set of invariant manifolds is present whether one is simulating steel, water or air. (Of course, there is a large number, typically $3NM = \infty$, of dimensions too!). More importantly, this becomes a powerful simulation tool if the atomic forces have a cut-off. One can simulate certain large-scale flows, or the failure of nanostructures, by a small simulation [11, 12]. One solves (20)-(21) merely for the simulated atoms, with forces given by all the atoms. Of course, this requires a good method for tracking some of the nonsimulated atoms, i.e., those within the cut-off. As a numerical method, this is called *objective molecular dynamics* [11].

Let us take a simple example, the translation group. Using a convenient indexing in terms of triples of integers $\nu = (\nu^1, \nu^2, \nu^3)$, we write $g_\nu = (I \,|\, a_\nu t + b_\nu)$. We see that to satisfy closure with this time-dependence, we must have

$$a_\nu t + b_\nu = \nu^1(\hat{b}_1 + \hat{a}_1 t) + \nu^2(\hat{b}_1 + \hat{a}_1 t) + \nu^3(\hat{b}_1 + \hat{a}_1 t) = \sum_{\ell=1}^{3} \nu^\ell (I + tA)e_\ell, \tag{25}$$

where $e_\ell = \hat{b}_\ell$ and the 3×3 matrix A is chosen so that $\hat{a}_\ell = A e_\ell$. Tacitly, we have assumed that the $e_\ell = \hat{b}_\ell$ are linearly independent, so that, initially, the atoms are not confined to a layer. The simulated atom positions are say $y_1(t), \ldots, y_M(t)$ and the nonsimulated atoms, $y_{\nu,k}(t) = g_\nu(y_k(t)) = y_k(t) + \nu^\ell (I + tA)e_\ell$, $\nu = (\nu^1, \nu^2, \nu^3) \in \mathbb{Z}^3, k = 1, \ldots, M$.

In this method atoms are moving around, filling space roughly uniformly. During computations, the simulated atoms quickly diffuse into the nonsimulated atoms. What is the macroscopic motion? We could spatially average the velocity, but that would be wrong: the velocity of continuum mechanics is not the average velocity of the particles! (For a simple explanation see [32].) To get the velocity of continuum mechanics we should average the momentum, and divide by the average density. Briefly, a suitable method in the present case is to prove that the center of mass of the simulated atoms moves with constant velocity which, by adding an overall Galilean transformation, we take to be zero[3]. Then the centers of mass of the images of the simulated atoms $g_\nu(y_k(t))$ then lie on a grid deforming according to the motion[4]

$$y(x,t) = (I + tA)x, \quad \text{or, in Eulerian form, } v(y,t) = A(I + tA)^{-1}y \tag{26}$$

---

[3]This requires an additional assumption on the forces $f_{i,k}$ that the resultant force on large volume, divided by the volume, tends to zero as the volume (at constant shape) goes to infinity [?]. This effectively rules out body forces, such as those due to gravity. It is easily proved directly for many accepted models of atomic forces.

[4]The Eulerian and Lagrangian forms are related by the parameterized ODE, $\partial y/\partial t = v(y(x,t),t)$, $y(0) = x \in \Omega \subset \mathbb{R}^3$.

Here, $v(y, t)$ is the velocity field. Note that by looking at the motions of centers of mass, we are precisely doing a spatial average of the momentum and then dividing by the average density. Given that we get to choose A, we get quite a few interesting motions. They can be very far-from-equilibrium, have nonzero vorticity (in fact, vortex stretching), and there are quite a few of both isochoric and non-isochoric examples.

Another interesting example is based on the (largest) Abelian helical group. In [11] it was used to study the failure of carbon nanotubes when stretched at constant strain rate.

5   Continuum and structural mechanics

Let's take the translation group, leading to (26). We have a macroscopic velocity field $v(y, t) = A(I + tA)^{-1}y$ arising from molecular dynamics simulation. For what choices of A, if any, does $v(y, t)$ satisfy some accepted equations of continuum mechanics? We can try the Navier-Stokes equations in the incompressible case. First we check that there are choices of A such that $\operatorname{div} v = 0$. It is easily[5] seen that $\operatorname{div} v = 0$ for $t > 0$ if and only if $\det A = \operatorname{tr} A = \operatorname{tr} A^2 = 0$, which, in turn implies that there is an orthonormal basis in which A has the form

$$ A = \begin{pmatrix} 0 & 0 & \kappa \\ \gamma_1 & 0 & \gamma_3 \\ 0 & 0 & 0 \end{pmatrix}. \tag{27} $$

(So, even for isochoric motions we can have a time-dependent vorticity, $\operatorname{curl} v = (\gamma_3 - \kappa\gamma_1 t, -\kappa, \gamma_1)$ in this basis.) Now substitute $v(y, t) = A(I + tA)^{-1}y$ into the Navier-Stokes equations

$$ \rho\left(\frac{\partial v}{\partial t} + \nabla v \, v\right) = -\nabla p + \Delta v, $$

$$ \text{i.e.,} \quad \rho(-A(I + tA)^{-1}A(I + tA)^{-1}y + A(I + tA)^{-1}A(I + tA)^{-1}y) = -\nabla p + 0, \tag{28} $$

so, with $p = const.$, the Navier-Stokes equations are identically satisfied.

The key properties being exploited in this case is that the left hand side of the balance of linear momentum is identically zero, and, for the right hand side, the stress is only a function of time when evaluated for the velocity field $v(y, t) = A(I + tA)^{-1}y$. So its divergence is zero. In fact, $v(y, t) = A(I + tA)^{-1}y$ identically satisfies the equations of all accepted models of fluid mechanics, including exotic models of non-Newtonian fluids and liquid crystals. The same is true of all accepted models of solid mechanics[6]. It is fascinating to observe that, despite the fact that molecular dynamics is time-reversible[7] and much of continuum mechanics is not time-reversible, this invariant manifold is inherited, in this sense, exactly.

Perhaps the most important feature of this family of solutions is that its form does not depend on the material. This is expected: as already noted, the invariant manifold of molecular dynamics (24) is also independent of the species of atoms being simulated. This feature

---

[5] Even easier, use the equivalent $\det(I + tA) = 1$ and write out the characteristic equation.

[6] It was advocated in [11] that a a fundamental requirement on models should be that $v(y, t) = A(I + tA)^{-1}y$ is a solution, i.e., that all continuum models inherit the invariant manifold.

[7] The function $y_{i,k}(-t)$ is a solution of (20) for initial conditions $y_{i,k}^\circ, -v_{i,k}^\circ$.

strikes to the heart of experimental science, especially experimental mechanics. If you want to learn about a material by testing it, you should impose boundary conditions that are at least consistent with *a possible solution of the governing equations*. But one does not know the coefficients of the governing equations ahead-of-time[8], because one has not yet measured the material properties! This fundamental dichotomy of experimental science is overcome by solutions of the type discussed here. Design the testing machine to produce boundary conditions consistent with a possible solution, and learn about the material by measuring the forces.

In fact, if one looks at the Couette viscometer in fluid mechanics or tension-torsion machine in solid mechanics, they do in fact, have a relation to these groups and their invariant manifolds. On the other hand these ideas could be more widely exploited in experimental science (e.g., [12]).

These were all purely mechanical cases. What happens when one adds thermodynamics? Let's return to the invariant manifold (24). In atomistic theory temperature is usually interpreted as mean kinetic energy based on the velocity obtained, importantly, after subtracting off the mean velocity. The temperature is then the mean kinetic energy of the simulated atoms, assuming, as we have done above, that the center of mass of the simulated atoms moves with zero velocity. But, unlike the velocity, there is nothing about a simulation based on (20) that would determine this temperature, beyond the expectation that it depends on A and the initial conditions (21) and, of course, the atomic forces. In simulations it can be rapidly changing, and, in fact, it is expected in some situations to go to infinity in finite time[9]. In summary, the temperature $\theta(t)$ is expected to be a function of time only, and not universal. The agrees with continuum theory, for which in most cases the energy equation reduces to an ODE for the temperature, when $v(y,t) = A(I + tA)^{-1}y$. In short, temperature is a function of time and its evolution is material dependent.

Experimental design is one of many subareas in continuum mechanics in which objective structures play an interesting role. Another is the blossoming area of structural mechanics called "origami structures"[10]. Fundamentally, frame-indifference is again being used: isometries take stress-free states to stress-free states.

Kawasaki's theorem in piecewise rigid origami concerns the $2n$-fold intersection. For example, in the ubiquitous case $2n = 4$, draw four lines on a piece of paper and fold along the lines[11]. This structure can be folded flat if and only if the sum of opposite angles is π. Without loss of generality $\hat{e}_1, \hat{e}_2, \hat{e}_3$ are orthonormal, the paper is the $\hat{e}_1, \hat{e}_2$-plane and consider fold-lines coming out of the origin in directions

$$
\begin{aligned}
t_1 &= \hat{e}_1, \quad t_2 = \cos\alpha\,\hat{e}_1 + \sin\alpha\,\hat{e}_2, \quad t_3 = \cos(\alpha+\beta)\hat{e}_1 + \sin(\alpha+\beta)\hat{e}_2, \\
t_4 &= \cos(\pi+\beta)\hat{e}_1 + \sin(\pi+\beta)\hat{e}_2,
\end{aligned}
\tag{29}
$$

corresponding to successive (sectors : angles) $(\mathcal{S}_1 : \alpha), (\mathcal{S}_2 : \beta), (\mathcal{S}_3 : \pi - \alpha), (\mathcal{S}_4 : \pi - \beta)$ with

---

[8]In cases on the cutting edge, one does not even know the form of the equations.

[9]See Section 6. Note that $(I + tA)$ can lose invertibility in finite time.

[10]Already, the link between architecture and molecular structure was articulated by Caspar and Klug [5]. See also [8]

[11]Or, simply crush a piece of paper and push down onto the table so it is flat. Upon unfolding, you will see numerous four-fold intersections with the sum of opposite angles equal to π. Even better, check many of the delightful folding arrangements discovered by Robert J. Lang and others [38].

$0 < \alpha, \beta < \pi$. Letting $t_i^\perp = Q_3 t_i$, $i = 1, \ldots, 4$, where Q_3 is a counter-clockwise rotation of $\pi/2$ with axis $\hat{e}_3$, it is easy to write down the folding deformation $y : \Omega \to \mathbb{R}^3$, with $0 \in \Omega \subset \mathbb{R}^2$:

$$
y(x) = \begin{cases}
x, & x \cdot \hat{e}_3 = 0, \ x \cdot t_2^\perp < 0, \ x \cdot t_1^\perp \geq 0, \\
R_2(\eta)x, & x \cdot \hat{e}_3 = 0, \ x \cdot t_3^\perp < 0, \ x \cdot t_2^\perp \geq 0, \\
R_2(\eta)R_3(\xi)x, & x \cdot \hat{e}_3 = 0, \ x \cdot t_4^\perp < 0, \ x \cdot t_3^\perp \geq 0, \\
R_2(\eta)R_3(\xi)R_4(\omega)x, & x \cdot \hat{e}_3 = 0, \ x \cdot t_1^\perp < 0, \ x \cdot t_4^\perp \geq 0,
\end{cases}
\tag{30}
$$

where $\eta = \pm\omega$ and

$$
\tan \xi = \begin{cases}
\frac{(\cos\alpha - \cos\beta)\sin\omega}{\cos\omega - \cos\alpha\cos\beta\cos\omega + \sin\alpha\sin\beta}, & \eta = \omega, \\[2mm]
\frac{(\cos\alpha + \cos\beta)\sin\omega}{\cos\omega + \cos\alpha\cos\beta\cos\omega - \sin\alpha\sin\beta}, & \eta = -\omega.
\end{cases}
\tag{31}
$$

Here $R_i(\theta) \in SO(3)$ has axis t_i and counter-clockwise angle θ, and $0 \leq \omega < \pi$ can be considered the homotopy parameter. We have fixed the overall rotation by putting $y(x) = x$ in $\mathcal{S}_1$[12]

Now we make a special choice of Ω: we choose it to be a general parallelogram, so that the fold-lines go from the origin to the corners. We have some freedom to assign angles and side lengths, as well as on the placement of the origin, but these restrictions can be easily organized. Now partially fold it, i.e., choose $\pm$ and a value of $0 < \omega < \pi$ in (30), (31). In the partly folded state let $\ell_1, \ell_2, \ell_3, \ell_4$ be consecutive edges on the boundary of the deformed parallelogram, so that $|\ell_1| = |\ell_3|$ and $|\ell_2| = |\ell_4|$. Choose two isometries $g_1 = (Q_1|c_1)$, and $g_2 = (Q_2|c_2)$ out of the air, arrange that they com-
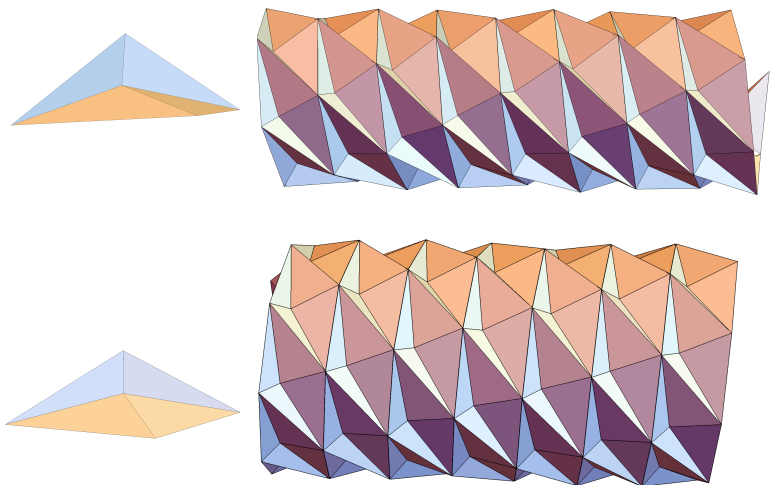

Figure 3: Helical origami structures generated by two commuting isometries whose powers give a discrete group. Bottom: the parallelogram is partly folded, as seen at left. Top: the same parallelogram is folded a little more. These solutions are isolated: for intermediate values of the homotopy parameter ω the associated group is not discrete.

mute, and arrange that $g_1(\ell_1) = \ell_3$ and $g_2(\ell_2) = \ell_4$. Of course, the latter is possible because g_1, g_2 are isometries, and there is obviously some freedom. This freedom is quantifiable without much difficulty. The underlying Abelian group is $\{g_1^i g_2^j : i, j \in \mathbb{Z}\}$.

Now we are done. The beauty of Abelian groups is that, not only does $g_1^i(y(\Omega))$, $i = 1, 2, \ldots$ produce a perfectly fitting helical origami chain, and $g_2^j(y(\Omega))$, $j = 1, 2, \ldots$ another such chain,

---

[12]In fact, this pair of homotopies, parameterized by $0 \leq \omega < \pi$ and $\pm$, are the only piecewise rigid deformations of Ω (with these fold lines) if $y(x) = x$ in $\mathcal{S}_1$ and $\alpha \neq \beta, \alpha + \beta \neq \pi$. If the latter holds there are some additional ones. The foldability of general arrays of 4-fold intersections, and a corresponding algorithm for folding them in terms of formulas like (30), is given in [39].

but also $g_1^i g_2^j (y(\Omega))$, $i, j = 1, 2, \ldots$ fills in the space between the chains perfectly with no gaps. See Figure 3.

However, Figure 3 is not the generic case. More typically, as i, j get large, the structure gets more and more complicated and begins to intersect itself. Of course, we knew that could happen because nothing above prevents self-intersections. But it is worse than that: there are accumulation points. The issue is: if we choose two commuting isometries "out of the air", invariably we will get a non-discrete group. Discreteness is a highly restrictive condition for isometry groups, and is the main force behind the structure of the crystallographic groups of
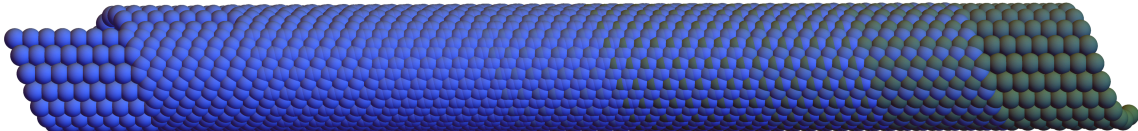

Figure 4: Orbit of a single blue ball under a subset of a nondiscrete Abelian group with two generators. The coloring is according to powers of one of these generators. Note that subsets of this structure coincide with structures that are locally 1-OS, 2-OS, etc.

the International Tables. It is nevertheless worth illustrating the appearance of the structure one gets. This is done in Figure 4 with balls instead of origami, for clarity. If one cuts off the powers i, j early enough, one gets a perfectly nice structure that in fact, at least with two generators, exhibits locally identical environments for most of the atoms. For that reason, these non-discrete groups – or more accurately, their generators – about which evidently we know nothing, are in fact quite interesting.

Moreover, orbits of non-discrete groups (with restricted powers) are seen in biology. Perhaps the most obvious example is the biologically important *microtubule*. Its structure is closely given by the construction above with two generators and carefully restricted powers[13]. Another interesting example is from the work of Reidun Twarock and collaborators [36, 29]. To understand the placement of receptors on the surface of a viral capsid, she takes the orbit of a certain non-discrete group with carefully restricted powers[14]. What are the nondiscrete isometry groups, and how do we restrict the powers of their generators in a rational way, perhaps guided by the concept of identical local environments?

In fact, one can satisfy all the matching conditions stated above using two commuting isometries that do generate a discrete group, and there are many choices. Figure 3 is an example. General theorems about these structures can be found in [18]. Beautiful origami structures that approximate an arbitrary Lipschitz map that shortens distances are given by Conti and Maggi [7].

Before moving on, it is worth highlighting the fundamental problem of self-intersection in origami structures, since it so often prevents foldability and there are no good methods to decide this ahead-of-time[15]. For mappings $y : \Omega \to \mathbb{R}^m$, $\Omega \in \mathbb{R}^n$, with $n = m$ a lot is known

---

[13]Its seam can be considered a consequence of non-discreteness and carefully restricted powers.

[14]To see that the generated group is not discrete in their simplest example (Figure 2 of [36]), let $g_1 = (I \,|\, t), g_2 = (R \,|\, 0)$ be the generators considered, where $R \in \mathrm{SO}(2)$ is a rotation of $\pi/5$ and $0 \neq t \in \mathbb{R}^2$. Then $g_3 := g_2 g_1 g_2^{-2} g_1 g_2 = (I \,|\, (2\cos(\pi/5))\, t)$. Thus g_1 and g_3 generate a nondiscrete subgroup because $2\cos(\pi/5) = (1/2)(1 + \sqrt{5})$ is irrational.

[15]Writing deformations in the form (30) – the continuum mechanics approach to origami structures – is a

that relates invertibility to invertibility on the boundary or to bounded measures of distortion [2, 6, 30]. The concept of global radius of curvature [26] has also been used for this purpose in knotted rods ($n = 1, m = 3$). Both of these approaches seem relevant, but neither seems ideally suited.

6 Boltzmann equation

We return to the family of invariant manifolds of the equations of molecular dynamics, which was seen to be inherited in a perfect way by continuum mechanics. We now consider statistical theories intermediate between molecular dynamics and continuum mechanics. Of greatest interest, in view of its remarkable predictive power in the far-from-equilibrium case, is the Boltzmann equation.

The Boltzmann equation [37, 43] is an evolution law for the molecular density function $f(t, y, v)$, $t > 0, y \in \mathbb{R}^3, v \in \mathbb{R}^3$, the probability density of finding an atom at time t, in small neighborhood of position y, with velocity v. It satisfies the Boltzmann equation:

$$\frac{\partial f}{\partial t} + v \frac{\partial f}{\partial x} = \mathbb{C}f(v) := \int_{\mathbb{R}^3} \int_{S^2} B\left(n \cdot \omega, |v - v_*|\right) \left[f' f'_* - f_* f\right] \, d\omega \, dv_*, \tag{32}$$

where S^2 is the unit sphere in $\mathbb{R}^3$, $n = n(v, v_*) = \frac{(v - v_*)}{|v - v_*|}$, (v, v_*) is a pair of velocities associated to the incoming collision of molecules and (v', v'_*) are outgoing velocities defined by collision rule

$$v' = v + ((v_* - v) \cdot \omega) \omega, \tag{33}$$
$$v'_* = v_* - ((v_* - v) \cdot \omega) \omega. \tag{34}$$

The form of the collision kernel $B\left(n \cdot \omega, |v - v_*|\right)$ is obtained from the solution of the two-body problem of dynamics with the given force law between molecules. We use the conventional notation in kinetic theory, $f = f(t, x, v)$, $f_* = f(t, x, v_*)$, $f' = f(t, x, v')$, $f'_* = f(t, x, v'_*)$.

Let A be any 3×3 matrix. We consider the translation group and the time-dependent invariant manifold specified by (24) with isometry group (25), macroscopic velocity $v(y, t) = A(I + tA)^{-1} y$, and a corresponding molecular dynamics simulation with atom positions $y_{\nu,k}(t)$, $\nu \in \mathbb{Z}^3, k = 1, \ldots, M$. At time t consider a ball $B_r(0)$ of any radius $r > 0$ centered at the origin, and another ball $B_r(y_\nu)$ of the same radius centered at $y_\nu = (I + tA)x_\nu$, where $x_\nu = \nu^1 e_1 + \nu^2 e_2 + \nu^3 e_3$. Both balls may contain some simulated atoms and some nonsimulated atoms. However, no matter how irregular the simulation, if I am given the velocities of atoms in $B_r(0)$ at time t, then I immediately know the velocities of atoms in $B_r(y_\nu)$ at time t. Specifically, if $v_1, \ldots, v_p$ are the velocities of atoms in $B_r(0)$, then $v_1 + Ax_\nu, \ldots, v_p + Ax_\nu$ are the velocities in $B_r(y_\nu)$. Or, in the Eulerian form appropriate to the Boltzmann equation, the velocities in $B_r(y_\nu)$ are

$$v_1 + A(I + tA)^{-1}y_\nu, \ldots, v_p + A(I + tA)^{-1}y_\nu. \tag{35}$$

---

reasonable step 1.

15

But $f(t, y, v)$ is supposed to represent the probability density of finding a velocity v in a small neighborhood of y. Therefore, we expect that this simulation corresponds to a molecular density function satisfying

$$f(t, 0, v) = f(t, y, v + A(I + tA)^{-1}y), \tag{36}$$

or, rearranging,

$$f(t, y, v) = g(t, v - A(I + tA)^{-1}y). \tag{37}$$

Substitution of (37) into the Boltzmann equation formally gives an immediate reduction: $g(t, w)$ satisfies

$$\frac{\partial g}{\partial t} - \left(A(I + tA)^{-1}w \right) \cdot \frac{\partial g}{\partial w} = \mathbb{C}g\left(w \right), \tag{38}$$

where the collision operator $\mathbb{C}$ is defined as in (32). Once, again, despite the Boltzmann equation being time-irreversible, the invariant manifold of molecular dynamics is inherited in the most obvious way. Note that at the level of the Boltzmann equation, periodicity has disappeared.

Equation (38) was originally found without reference to molecular dynamics, but rather by noticing similarities between special solutions of equations of fluid mechanics and the moment equations[16] of the kinetic theory [24, 41]. Recently, an existence theorem for (38) has been given [33], with surprising implications for the invariant manifold.

The most explicit results are for *Maxwellian molecules*. These are molecules that attract with a force proportional to the inverse 5th power of their separation. For the collision kernel B appropriate to these molecules the invariance of the left and right hand sides of (32) or (38) match. We focus on the entropy (minus the H-function) given by

$$\eta(t) = -\int_{\mathbb{R}^3} g(t, w) \log g(t, w)\, dw. \tag{39}$$

The asymptotic analysis of self-similar solutions [33] gives, for a large class of choices of A,

$$\eta(t) = \rho(t) \log \left(\frac{e(t)^{3/2}}{\rho(t)} \right) + C_g, \tag{40}$$

where the density ρ and temperature e are given by explicit formulas:

$$\rho(t) = \int_{\mathbb{R}^3} g(t, w)\, dw, \quad e(t) = \int_{\mathbb{R}^3} \frac{1}{2} w^2 g(w, t)\, dw, \tag{41}$$

and C_g is constant. In these far-from-equilibrium solutions the temperature and density can be rapidly changing, and the entropy rapidly increasing. Nevertheless, the relation (40) between entropy, density and temperature expressed by (40) *is the same as for the equilibrium Maxwellian distribution.* That's true except for one small but interesting point: the constant C_g is strictly less than that of the Maxwellian distribution. From an information theoretic viewpoint, the uncertainty of positions and velocities of atoms on the invariant manifold differs from those of an equilibrium state at the same temperature and density by a constant, even as the temperature evolves rapidly to infinity.

---

[16]Multiply (38) by polynomials in w and integrate over $\mathbb{R}^3$. The study of the solutions of the moment equations has an extensive history beginning with Galkin [24] and Truesdell [41] and reviewed in [42]

7 Maxwell's equations

Maxwell's equations have a bigger invariance group, the Lorentz group[17] of special relativity. It would be interesting to have a look at this full group, but we shall confine attention to its Euclidean subgroup of isometries. The solutions of Maxwell's equations do not describe matter itself, but they interact with matter. In fact, almost everything we know about the structure of matter comes by interpreting this interaction. This interpretation is not straightforward because, at the relevant wavelengths, we cannot measure the scattered electric or magnetic fields directly, but only the time average of the magnitude of their cross product[18]. Nevertheless, increasingly, such as in quasicrystals, the classification of atomic structures is *defined* in terms of this interaction.

Even in the case of the now accepted definition of quasicrystals, the incoming radiation is plane waves. That is, we assign electric and magnetic fields, respectively,

$$E(y,t) = n e^{i(k \cdot y - \omega t)} \quad \text{and} \quad B(y,t) = \frac{1}{\omega}(k \times n) e^{i(k \cdot y - \omega t)}, \tag{42}$$

where $n \in \mathbb{C}^3$, $k \in \mathbb{R}^3$, $k \cdot n = 0$, $\omega = c|k|$ and c is the speed of light. These plane waves exert a force $e(E + v \times B)$ on each electron of the structure, which vibrates with velocity v. Moving charges generate electromagnetic fields and so, the vibrating electrons, each with charge e, send out spherical waves which in the far-field are again approximately plane waves. The rigorous asymptotics of this process is delicate [22] and involves several small parameters in addition to the Fresnel number $\mathrm{dia}(\Omega)^2|k|/d \ll 1$. Here $\Omega \subset \mathbb{R}^3$ is the illuminated region, and d is the distance to the detector. The results are formulas in terms of $E_0(y) = n e^{ik \cdot y}$ for the electric and magnetic fields in the far-field:

$$
\begin{aligned}
E_{out}(y,t) &= -c_{e\ell} \frac{e^{i(k'(y) \cdot y - \omega t)}}{|y - y_c|} \left(I - \frac{k'(y)}{|k'(y)|} \otimes \frac{k'(y)}{|k'(y)|} \right) \int_\Omega E_0(z) \rho(z) \, e^{-ik'(y) \cdot z} dz, \\
B_{out}(y,t) &= \frac{1}{\omega} k'(y) \times E_{out}(y,t),
\end{aligned}
\tag{43}
$$

where $\rho : \mathbb{R}^3 \to \mathbb{R}^{\geq}$ is the electronic density, $x_c \in \Omega$ is a typical point of the illuminated region, c_{el} is a universal constant depending on the charge and mass of an electron, and

$$k'(y) = \frac{\omega}{c} \frac{y - y_c}{|y - y_c|}. \tag{44}$$

With a simple idealized example we can begin to understand plane wave X-ray methods. In the notation of Section 2, we assume that the electronic density is a sum of Dirac masses at the points of a Bravais lattice generated by the linearly independing vectors e_1, e_2, e_3,

$$\rho(y) = \sum_{z \in \mathcal{L}(e_1, e_2, e_3) \cap \Omega} \delta_z(y). \tag{45}$$

With this choice the integral in (43) is

$$\int_\Omega n e^{ik \cdot z} \rho(z) \, e^{-ik'(y) \cdot z} dz = \sum_{z \in \mathcal{L}(e_1, e_2, e_3) \cap \Omega} n \, e^{-i((k'(y) - k) \cdot z)}. \tag{46}$$

---

[17]in fact, the conformal Lorentz group, which includes dilatations as well as Lorentz transformations [4].

[18]that is, the time average of the Poynting vector (see [21], p. 1196).

17

Therefore, if $k'(y) - k$ belongs to the reciprocal lattice $\mathcal{L}(e^1, e^2, e^3)$, $e^i \cdot e_j = 2\pi \delta_j^i$, then the exponential factor contributes 1 to the (complex[19]) magnitude of (46) for every lattice point: that is, constructive interference.

How much of this constructive interference is a consequence of choosing the electronic density to be a sum of Dirac masses? Almost nothing [21, 20]: *Suppose instead we assume*

$$\rho_r(y) = \sum_{z \in \mathcal{L}(e_1, e_2, e_3),\, |z| < r} \varphi(y - z) \tag{47}$$

for a smooth function $\varphi : \mathbb{R}^3 \to \mathbb{R}^{\geq}$ with compact support, or, more generally, in the Schwartz class $\mathcal{S}(\mathbb{R}^3)$. Here we have chosen $\Omega = B_r(0)$ as the illuminated region. Then, the limit in the sense of distributions of the complex magnitude of the integral in the expression (43) for E_{out} is

$$\lim_{r \to \infty} \left| \int_{B_r(0)} E_0(z) \rho(z)\, e^{-ik'(y) \cdot z} dz \right| = \sum_{z' \in \mathcal{L}(e^1, e^2, e^3)} |\hat{\varphi}(z')|\, \delta_{z'}(k'(y) - k). \tag{48}$$

From this result we not only see constructive interference but also strong destructive interference: the sum in (48) is zero when $k'(y) - k$ does not belong to the reciprocal lattice. It is this result that underlies the 2 to 4 order-of-magnitude difference between peak heights and background, and the sharpness of the peaks, in X-ray methods. This in turn is what makes this method so accurate for structure determination. Discovery, improvement and application of the method has led to no less than 14 Nobel prizes.

All this works because of matching symmetries. In the calculation (46) it is the ability to combine the phase factors, or more precisely, that the translation group acting on plane waves gives a phase factor times the plane wave back again. For more general choices of ρ, we can use translation invariance (up to the multiplicative phase factor) of $\rho(z)$ on the left hand side of (46) to condense the integral to a lattice sum of an integral over the unit cell, to see constructive interference. A more powerful method is the italicized theorem just above, which is proved by a direct application of the Poisson summation formula [21]. The property of plane waves being used is, for the translation $g_c = (I \,|\, c)$,

$$g_c(n e^{ik \cdot y}) := n e^{ik \cdot (y + c)} = e^{ik \cdot c}(n e^{ik \cdot y}), \tag{49}$$

i.e., with the group action indicated on the left of (49), the plane wave $n e^{ik \cdot y}$ is an eigenfunction of the translation group. The eigenvalues $e^{ik \cdot c}$ are the characters of this Abelian group. The two key mathematical properties of plane waves are that, with the natural action (49), (i) they are eigenfunctions of the translation group and (ii) they are solutions of Maxwell's equations.

So much for plane waves. In principle, everything should work in the same way for any other Abelian isometry group G. As seen in Section 2 and elsewhere, many of the most studied structures today are not crystals, and it would be good to have an accurate method of structure determination for them. Perhaps the most interesting mathematically are helical structures like single-walled carbon nanotubes[20]. For one, the helical groups do not fit the

---

[19]Ibid. The time average of the Poynting vector for time-harmonic radiation is, up to a constant factor, the complex magnitude of the electric field in the time harmonic case.

[20]Due to the issues discussed here and the typical presence of mixed chiralities in samples, the lattice parameters of carbon nanotubes are not accurately known.

classification scheme of the International Tables of Crystallography – there are infinitely many helical groups according to that scheme. For another, helical (as well as many other) structures tend to resist crystallization. Third, even if helical structures can be crystallized, it is quite unclear that the structure will be close to the native structure.

We shall consider time harmonic solutions of Maxwell's equations: $E(y,t) = E_0(y)e^{-i\omega t}$, $B(y,t) = B_0(y)e^{-i\omega t}$, $E_0 : \mathbb{R}^3 \to \mathbb{C}^3$, $B_0 : \mathbb{R}^3 \to \mathbb{C}^3$. In this case Maxwell's equations become

$$\Delta E_0 = -\frac{\omega^2}{c^2}E_0, \quad \text{div } E_0 = 0, \quad B_0 = -\frac{i}{\omega}\text{curl}E_0. \tag{50}$$

For time-harmonic radiation the electric and magnetic fields in the far-field are still given by (43), but now for a solution $E_0(y)$ of (50).

A critical part is choosing the action so that (i) is nontrivial and (ii) exploits the invariance of Maxwell's equations. The right action is

$$\text{for } g = (Q\,|\,c) \in G, \quad g[E](y,t) = QE(g^{-1}(y),t) = QE(Q^T(y-c),t). \tag{51}$$

Here we use the bracket notation [...] to distinguish the action from that already introduced, $g(y) = Qy + c$. Summarizing, we have *design equations*:

$$(i) \text{ for all } g \in G, \ g[E_0] = \chi_g E_0, \text{ and } \quad (ii) \ E_0 \text{ satisfies Maxwell's equations (50)}. \tag{52}$$

Of course, plane waves satisfy the design equations.

The largest (discrete) Abelian helical group is

$$\{h^i g^j : i \in \mathbb{Z}, \ j = 1, \dots, n\} \text{ where } h = (R_\theta\,|\,\tau e), \ g = (R_{2\pi/n}\,|\,0). \tag{53}$$

with $R_\psi \in \text{SO}(3)$ having angle ψ and axis through e, $|e| = 1$, $0 < \theta < 2\pi$ and[21] $n \in \mathbb{N}$.

Exploiting (52) for the helical group (53) is quite easy if we begin with (i). First, the eigenvalue χ_g, $g \in G$, is seen to be a bounded continuous homomorphism from G to $\mathbb{C} \setminus 0$ under multiplication in $\mathbb{C}$, and therefore a character of G. The characters are $\chi_g = \chi(\theta, \tau) = e^{i(\alpha\theta + \beta\tau)}$, $\alpha \in \mathbb{Z}, \beta \in \mathbb{R}$. Then, one can easily find the general form of E_0 satisfying (i): in cylindrical coordinates (r, φ, z) this is $E_0(r, \varphi, z) = e^{i(\alpha\varphi + \beta z)}R_\varphi E_0(r, 0, 0)$. Finally, substitution of the latter into Maxwell's equations reduces them to a solvable system of ODEs. A general form of the result are *twisted waves*[22]:

$$E(y,t) = \frac{1}{2\pi}e^{-i\omega t}\int_{-\pi}^{\pi} e^{i\alpha\psi}R_\psi n \, e^{i\,y\cdot R_\psi k}d\psi, \quad k = (0, \gamma, \beta). \tag{54}$$

Here, $n \in \mathbb{C}^3$ satisfies $n \cdot k = 0$. A picture of a twisted wave is shown in Figure 5.

Theoretically, twisted waves can be used for structure determination of helical structures similar to the way plane waves are used on periodic structures. A complete scheme for theoretical structure determination is proposed in [21, 35]. The key parameters that are varied are α and β. We cannot describe this in detail here, but one can get a glimpse of the idea from Figure 6. Suppose we have an helical objective structure as shown in 6a. We are looking

---

[21]Strictly speaking, to be a helical group, θ is an irrational multiple of 2π but we will not need this restriction.
[22]For the form given here, see [34]; for alternative expressions see [35].
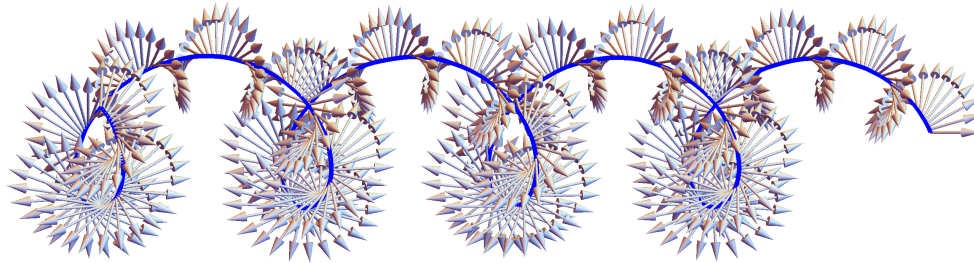
Figure 5: A twisted wave showing electric field vectors plotted along an integral curve (blue) of the Poynting vector.

down the axis. Each yellow atom sees the same environment; each red atom sees the same environment; each green atom sees the same environment. In 6b we have superposed on this structure a twisted wave whose values of α, β, n are tuned to give constructive interference, and we have plotted just the electric field vectors at the atoms. As one can see, all the red vectors are parallel, all the green vectors are parallel, and all the yellow vectors are parallel in this
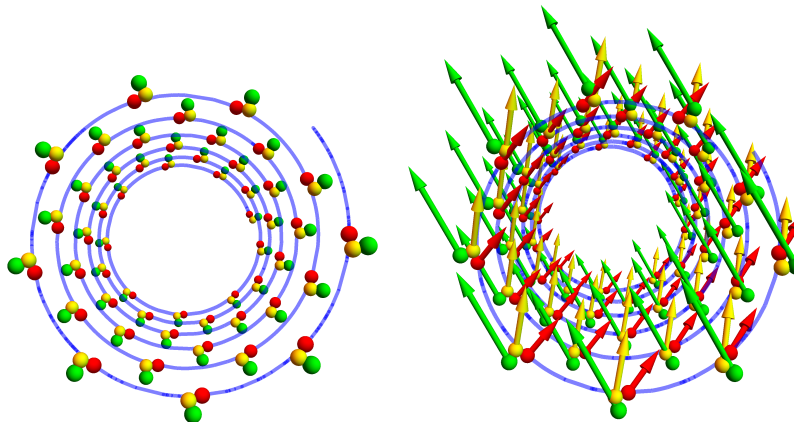
(a) A 3-OS   (b) 3-OS with twisted wave

Figure 6: (a) A 3-OS with green, yellow and red atoms, viewed down the axis. (b) The same structure with a superimposed twisted wave highlighted at the atom positions.

projection. One can imagine that, if the phases are properly tuned one can get constructive interference, measured at a detector on the axis. Moreover, the different length vectors should in fact give information about what is in the unit cell.

These pictures illustrate constructive interference. Destructive interference that occurs when the parameters or structure is tuned slightly off resonance relies on a far reaching generalization of the Poisson summation formula [44] which in turn requires that the group be extendable to a continuous symmetry group. In the case of the helical group this generalization can also be seen in a simpler way [21].

8 Perspective

Clearly the subject of structure and invariance has a ragged boundary! Some questions that could have been considered a century ago seem not to have been asked, and simple questions

posed then seem to be excruciatingly difficult. But the subject has a vibrant connection with materials science and technology today, with links to nanoscience, quasicrystals, origami, structure determination and multiscale mathematics. In this section we make a selection of what are (to the author) intriguing mathematical problems related to this line of thinking.

The most fundamental question seems to us to be: why do elements in the Periodic Table, and nanostructures made with one element, having widely differing atomic forces and bonding patterns, choose to crystallize as objective structures? Can that be proved in some framework, while initially avoiding the question of what is the detailed structure?

There is an intriguing link between subsets of nondiscrete groups of isometries, objective structures and quasicrystals. What are these groups, and how does one rationally choose the subsets. Does this lead to a more physically-based approach to quasicrystalline structures than the projection method?

Seeking some kind of general nonequilibrium statistical mechanics, that has something like the simplicity of equilibrium statistical mechanics, is in the author's view hopeless. After all, even the Boltzmann equation treats only the more rudimentary kind of material, and it has all the complexity of a general initial-value problem of a nonlinear integro-differential equation for a function of 7 variables. A classic approach is to try to simplify by looking near equilibrium. A fresh approach could be the following. We have followed a far-from-equilibrium invariant manifold from molecular dynamics to the Boltzmann equation to continuum mechanics. There seem to be many coincidences, such as an explicit relationship between density, temperature and entropy that holds far from equilibrium. These are highly suggestive that there may be a relatively simple statistical mechanics *on this manifold*. There the only gradient is the velocity gradient. Of course, any such statistical mechanics cannot be based on Hamiltonian $= const.$.

The method of objective molecular dynamics presented in Section 4 could be more widely used. There are also fundamental mathematical questions (stability) and subtle numerical issues (efficiency). Note that in a general continuum flow, a piecewise constant spatial approximation of the Lagrangian velocity field nominally gives a set of elements each with a constant A. Is there a general multiscale method here?

What is the scope of the interaction light with matter? For example, even though the structure in Figure 4 is not the orbit of a discrete group of isometries, it seems likely that, with the right radiation, we could get a pretty strong constructive interference from it.

And finally, like a lot of mathematics, the key to understanding origami seems to be rigidity. But, established lines of thinking about rigidity in differential geometry or elasticity seem not to be fruitful. On the other hand, the link between martensitic phase transformations and origami, already pioneered by Conti and Maggi [7], seems to be highly suggestive.

References

[1] Edgar C. Bain. The nature of martensite. *Trans. AIME*, 70(1):25, 1924.

[2] John M. Ball. Global invertibility of Sobolev functions and the interpenetration of matter. *Proceedings of the Royal Society of Edinburgh Section A: Mathematics*, 88(3-4):315–328, 1981.

[3] Amartya S Banerjee, Ryan S Elliott, and Richard D James. A spectral scheme for kohn–sham density functional theory of clusters. *Journal of Computational Physics*, 287:226–253, 2015.

[4] Harry Bateman. The transformation of the electrodynamical equations. *Proceedings of the London Mathematical Society*, 2(1):223–264, 1910.

[5] Donald L. D. Caspar and Aaron Klug. Physical principles in the construction of regular viruses. In *Cold Spring Harbor symposia on quantitative biology*, volume 27, pages 1–24. Cold Spring Harbor Laboratory Press, 1962.

[6] Philippe G. Ciarlet and Jindřich Nečas. Injectivity and self-contact in nonlinear elasticity. *Archive for Rational Mechanics and Analysis*, 97(3):171–188, 1987.

[7] Sergio Conti and Francesco Maggi. Confining thin elastic sheets and folding paper. *Archive for Rational Mechanics and Analysis*, 187(1):1–48, 2008.

[8] H. S. M. Coxeter. Virus macromolecules and geodesic domes. *A spectrum of mathematics*, pages 98–107, 1971.

[9] H. R. Crane. Principles and problems of biological growth. *The Scientific Monthly*, 70(6):376–389, 1950.

[10] Francis H. C. Crick and James D. Watson. Structure of small viruses. *Nature*, 177(4506):473–475, 1956.

[11] Kaushik Dayal and Richard D. James. Nonequilibrium molecular dynamics for bulk materials and nanostructures. *Journal of the Mechanics and Physics of Solids*, 58(2):145 – 163, 2010.

[12] Kaushik Dayal and Richard D. James. Design of viscometers corresponding to a universal molecular simulation method. *Journal of Fluid Mechanics*, 691:461–486, 2012.

[13] Nikolai P. Dolbilin, J. C. Lagarias, and Marjorie Senechal. Multiregular point systems. *Discrete & Computational Geometry*, 20(4):477–498, 1998.

[14] Traian Dumitrica and Richard D. James. Objective molecular dynamics. *Journal of the Mechanics and Physics of Solids*, 55(10):2206 – 2236, 2007.

[15] J. L. Ericksen. Special topics in elastostatics. In C.-S. Yih, editor, *Advances in Applied Mechanics*, volume 17, pages 189–244. Academic Press, 1977.

[16] Leonhard Euler. Recherches physiques sur la nature des moindres parties de la matière. *Berlin Academy Memoires*, 1:28–32, 1745. (*Opera omnia*, III. 1: 615).

[17] Wayne Falk and Richard D. James. Elasticity theory for self-assembled protein lattices with application to the martensitic phase transition in bacteriophage t4 tail sheath. *Physical Review E*, 73(1):011917, 2006.

[18] Fan Feng, Paul Plucinsky, and Richard D. James. Phase transformations in helical structures. Preprint, 2017.

[19] L. C. Flatley and Florian Theil. Face-centered cubic crystallization of atomistic configurations. *Archive for Rational Mechanics and Analysis*, 218(1):363–416, 2015.

[20] Gero Friesecke. *Lectures on Fourier Analysis*. University of Warwick, Coventry, UK, 2007.

[21] Gero Friesecke, Richard D. James, and Dominik Jüstel. Twisted x-rays: incoming waveforms yielding discrete diffraction patterns for helical structures. *SIAM Journal on Applied Mathematics*, 76(3):1191–1218, 2016.

[22] Gero Friesecke, Richard D. James, and Dominik Jüstel. The far-field intensity in kinematic x-ray diffraction for general incoming radiation. Preprint, 2017.

[23] Gero Friesecke and Florian Theil. Validity and failure of the cauchy-born hypothesis in a two-dimensional mass-spring lattice. *Journal of Nonlinear Science*, 12(5), 2002.

[24] V. So. Galkin. On a class of solutions of grad's moment equations. *Journal of Applied Mathematics and Mechanics*, 22(3):532–536, 1958. (Russian version, *PMM* **20**, 445-446, (1956)).

[25] Clifford S. Gardner and Charles Radin. The infinite-volume ground state of the Lennard-Jones potential. *Journal of Statistical Physics*, 20(6):719–724, 1979.

[26] Oscar Gonzalez and John H Maddocks. Global curvature, thickness, and the ideal shapes of knots. *Proceedings of the National Academy of Sciences*, 96(9):4769–4773, 1999.

[27] D. Hobbs, J. Hafner, and D. Spišák. Understanding the complex metallic element Mn. I. Crystalline and noncollinear magnetic structure of α-Mn. *Physical Review B*, 68(1):014407, 2003.

[28] Robert Hooke. *Micrographia: or, Some physiological descriptions of minute bodies made by magnifying glasses.* J. Martyn and J. Allestry, London, first edition, 1665.

[29] Giuliana Indelicato, Tom Keef, Paolo Cermelli, David G. Salthouse, Reidun Twarock, and Giovanni Zanzotto. Structural transformations in quasicrystals induced by higher dimensional lattice transitions. In *Proc. R. Soc. A*, volume 468, pages 1452–1471. The Royal Society, 2012.

[30] Tadeusz Iwaniec, Leonid V. Kovalev, and Jani Onninen. Diffeomorphic approximation of Sobolev homeomorphisms. *Archive for rational mechanics and analysis*, 201(3):1047–1067, 2011.

[31] Richard. D. James. Objective structures. *Journal of the Mechanics and Physics of Solids*, 54(11):2354–2390, 2006.

[32] Richard D. James. Continuum mechanics. In Mark R. Dennis, Paul Glendinning, Paul A. Martin, Fadil Santosa, and Jared Tanner, editors, *The Princeton Companion to Applied Mathematics*, pages 446–458. Princeton University Press, 2015.

[33] Richard D. James, Alessia Nota, and Juan J. L. Velázquez. Self-similar profiles for homoenergetic solutions of the Boltzmann equation: particle velocity distribution and entropy. *arXiv preprint arXiv:1710.03653*, 2017.

[34] D. Jüstel. *Radiation for the analysis of molecular structures with non-crystalline symmetry: modelling and representation theoretic design*. PhD thesis, Technical University of Munich, 2014.

[35] Dominik Jüstel, Gero Friesecke, and Richard D. James. Bragg–von laue diffraction generalized to twisted x-rays. *Acta Crystallographica Section A: Foundations and Advances*, 72(2):190–196, 2016.

[36] Thomas Keef, Jessica P. Wardman, Neil A. Ranson, Peter G. Stockley, and Reidun Twarock. Structural constraints on the three-dimensional geometry of simple viruses: case studies of a new predictive tool. *Acta Crystallographica Section A: Foundations of Crystallography*, 69(2):140–150, 2013.

[37] James Clerk Maxwell. On the dynamical theory of gases. *Philosophical transactions of the Royal Society of London*, 157:49–88, 1867.

[38] Koryo Miura, Toshikazu Kawasaki, Tomohiro Tachi, Ryuhei Uehara, Robert J. Lang, and Patsy Wang-Iverson. *Origami^6: I. Mathematics*. American Mathematical Society, 2015.

[39] Paul Plucinsky, Fan Feng, and Richard D. James. An algorithm to generate all possible generalized miura origami. Preprint, 2017.

[40] Florian Theil. A proof of crystallization in two dimensions. *Communications in Mathematical Physics*, 262(1):209–236, 2006.

[41] C. Truesdell. On the pressures and the flux of energy in a gas according to maxwell's kinetic theory, ii. *Journal of Rational Mechanics and Analysis*, 5(1):55–128, 1956.

[42] Clifford Truesdell and Robert G Muncaster. *Fundamentals of Maxwell's Kinetic Theory of a Simple Monatomic Gas*, volume 83. Academic Press, 1980.

[43] Cédric Villani and Clément Mouhot. Kinetic theory. In Mark R. Dennis, Paul Glendinning, Paul A. Martin, Fadil Santosa, and Jared Tanner, editors, *The Princeton Companion to Applied Mathematics*, pages 446–458. Princeton University Press, 2015.

[44] André Weil. Sur certains groupes d'opérateurs unitaires. *Acta mathematica*, 111(1):143–211, 1964.